

# Control of optical chaos spectrum in semiconductor laser for secure RoF communication

DANISH ALI MAZHAR<sup>1</sup>, SYED ZAFAR ALI<sup>2</sup>, MUHAMMAD KHAWAR ISLAM<sup>3</sup>

<sup>1</sup>Department of Telecommunication Engineering, UET, Taxila, Pakistan

<sup>2</sup>Department of Electrical Engineering, Air University, Islamabad, Pakistan

<sup>3</sup>Department of Electrical Engineering, Taibah University, AL Madinah Al Munawarah, KSA

A critical requirement in optical chaos based secure radio over fiber (RoF) system design is the ability to control center frequency, spectral bandwidth, power level and signature of chaos to submerge message with sufficient horizontal and vertical margins both in time and frequency domains. Once frequency domain masking is completely achieved, time domain masking is met automatically, the former being more stringent. In a direct modulated semiconductor laser, the three control parameters are bias current ( $I_{bias}$ ), modulation current ( $I_{mod}$ ) and modulation frequency ( $\omega_a$ ). It is found that  $I_{mod}$  increases bandwidth and amplitude dynamic range of chaotic pulses.  $I_{bias}$  increases the cavity power and hence average peak amplitude of laser chaotic pulses. The modulation frequency increases the speed of overall cavity dynamics and hence is used to increase the bandwidth of chaos but a corresponding increase in bias and modulation currents is required to support high repetition pulses. The results show relationship between three control parameters (bias current, modulation current and modulation frequency) in a direct modulated semiconductor laser and optical chaos bandwidth using regression.

Keywords: chaos, radio over fiber, secure optical communication.

## 1. Introduction

Chaos is ubiquitously found in both naturally existing and man-made complex nonlinear systems. The human heart pulsed ECG and human brain pulsed neuron signals are also inherently chaotic, specifically like the spiky or pulsed chaos produced by both semiconductor [1-5] and fiber lasers [6-10]. This fact emphasizes the importance of studying pulsed chaos in time domain, RF and optical spectral domains in this work. The intended application here is secure RoF communication, yet due to rich dynamics studied very systematically, this work may have further applications of interest in related areas. Optical chaos has been studied both numerically and experimentally for three decades in an effort to ensure physical layer security of analog and digital optical communication and EU funded field demonstration in Athens [2] has demonstrated the working of overall concept. Chaos is generated in both continuous nonlinear and dis-

crete systems with certain system configuration, parameter range and specific driving conditions. Chaos is not only sensitive to initial conditions but also to system parameters and external driving conditions in non-autonomous cases.

Radio over fiber (RoF) is enabling technology as more and more radar and radio short links are getting transferred [11-14] to RoF due to its immunity to noise and interference. Combining optical chaos with RoF is a promising new research area, and we have shown [1] how the benefits of the two fields can be combined to achieve secure RoF in analog and digitized RoF scenarios. This particular study is a next logical step in one our work in which we investigate how direct modulated laser diode chaos bandwidth and power are controllable by three driving signal parameters *i.e.*,  $I_{\text{bias}}$ ,  $I_{\text{mod}}$  and  $\omega_a$ . This study will help in solving two aspects of RoF masking in optical chaos signal. Firstly, what ranges are required for RoF signal center frequency, band width and spectral power profile for a given optical chaos spectrum. Secondly, what laser diode driving parameters shall be chosen for a given RoF signal with sufficient margins in frequency and power. Chaos bandwidth study of semiconductor laser has been conducted previously and reported in literature [15-18] in few other configurations. This work is is a comprehensive study of directly modulated semiconductor laser.

## 2. Mathematical model

The mathematical model for direct modulation of semiconductor lasers is given in Eqs. (1)-(2) and parameter values are given in the Table. It may be noted that same direct modulated laser model can be used both for RF to optical signal conversion in RoF application and generation of optical chaos. However, due to the nonlinearities of laser diode and subsequent THD, a Mach-Zehnder modulator is preferred over laser diode for former purpose and here only latter application is under study.  $I_{\text{bias}}$  is the dc bias current to set the  $Q$  point of laser diode above the threshold current ( $I_{\text{th}}$ ).  $I_{\text{mod}}(t)$  is the RF modulation current added to the bias current and is a sinusoidal wave in 1–15 GHz range for this study.  $G(N, S)$  is the optical gain coefficient,  $\varepsilon$  is the mode confinement factor of the cavity ranging between 0 and 1,  $d$  is the thickness of active

Table. System parameters for chaos generation.

Parameters	Values
Laser frequency	193.1 THz
Power at bias current	1 mW
Modulating sine wave frequency	4–15 GHz
Active layer volume $V$	$0.15 \times 10^{-9} \text{ cm}^3$
Mode confinement factor $\varepsilon$	0.4
Carrier lifetime $\gamma_s$	$1 \times 10^{-9} \text{ sec}$
Photon lifetime $\gamma_c$	$3 \times 10^{-12} \text{ sec}$
Carrier density at transparency	$1 \times 10^{18} / \text{cm}^3$
Threshold current	33.45 mA
Threshold power	0.015 mW

layer of the laser which further decides the active volume of the cavity.  $\gamma_c$  is photon decay rate and  $\gamma_s$  is spontaneous carrier decay rate.

$$\frac{dS}{dt} = -\gamma_c N + \varepsilon G(N, S)S \quad (1)$$

$$\frac{dN}{dt} = -\gamma_c S - G(N, S)S + \frac{I_{\text{bias}} + I_{\text{mod}}}{Ve} \quad (2)$$

### 3. Simulations

Extensive simulations have been carried out for three main control parameters, *i.e.* modulation current  $I_{\text{mod}}$ , bias current  $I_{\text{bias}}$  and modulation frequency  $\omega_a$ . Two types of results have been collected and shown, *i.e.* simulation results and statistically analyzed results. For simulation results, three types of plots have been generated for each variation in parameter, *i.e.* time domain plot, optical spectrum plot and RF spectrum plot. The three mentioned parameters are kept within a range such that the laser diode maintains its chaotic range of operation. Therefore, trend analysis of chaos can be done in terms of bifurcation behavior, mean, standard deviation and RF/optical bandwidth of chaos.

#### 3.1. Modulation current $I_{\text{mod}}$

The ratio of  $I_{\text{mod}}$  and  $I_{\text{bias}}$  is defined as modulation depth  $m_a$ . All other parameters are kept as per the Table and only modulation current is increased from 40 to 400 mA, thereby increasing modulation depth from 1 to 10. The variation of time domain, optical frequency, and RF spectrum plots with  $I_{\text{mod}}$  and consequently  $m_a$  is shown in Fig. 1. It is observed that the chaos bandwidth in optical and RF domains increases with modulation current and modulation index. Also, the time domain plots show that

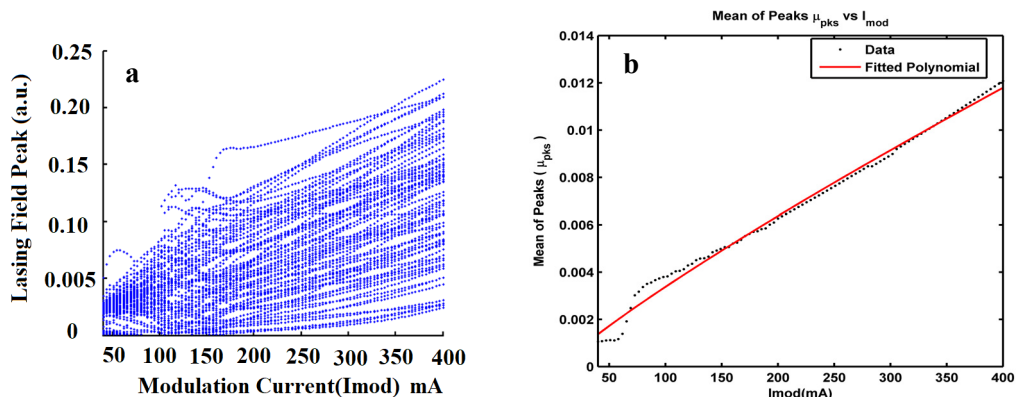


Fig. 1. Chaotic peaks variation with  $I_{\text{mod}}$ : (a) Bifurcation plot, (b) mean power, (c) standard deviation, (d) optical 10 dB bandwidth.

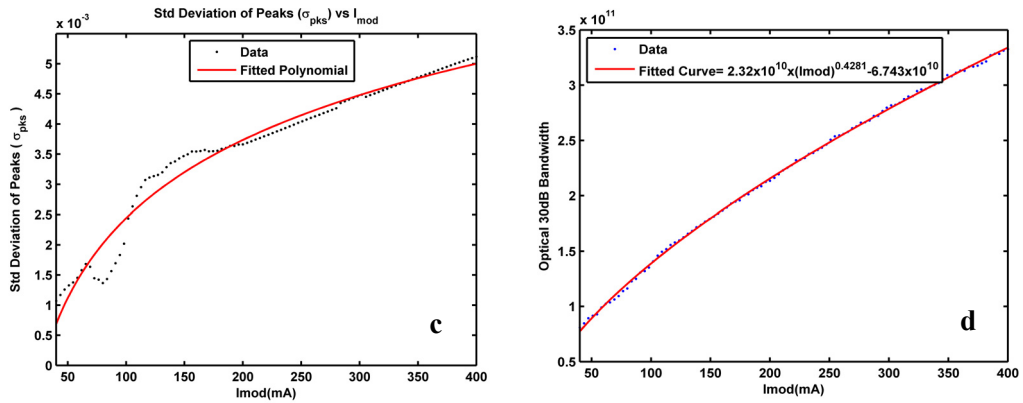


Fig. 1. Continued.

the average peak amplitude and dynamic range of chaos pulses are less for small modulation current of 40 mA as shown in Fig. 1**a**. Both these quantities rise as the modulation current is increased as was obvious in bifurcation diagram of Fig. 2**a** as well. So, in this case bandwidth correlates directly to dynamic range of chaotic pulses.

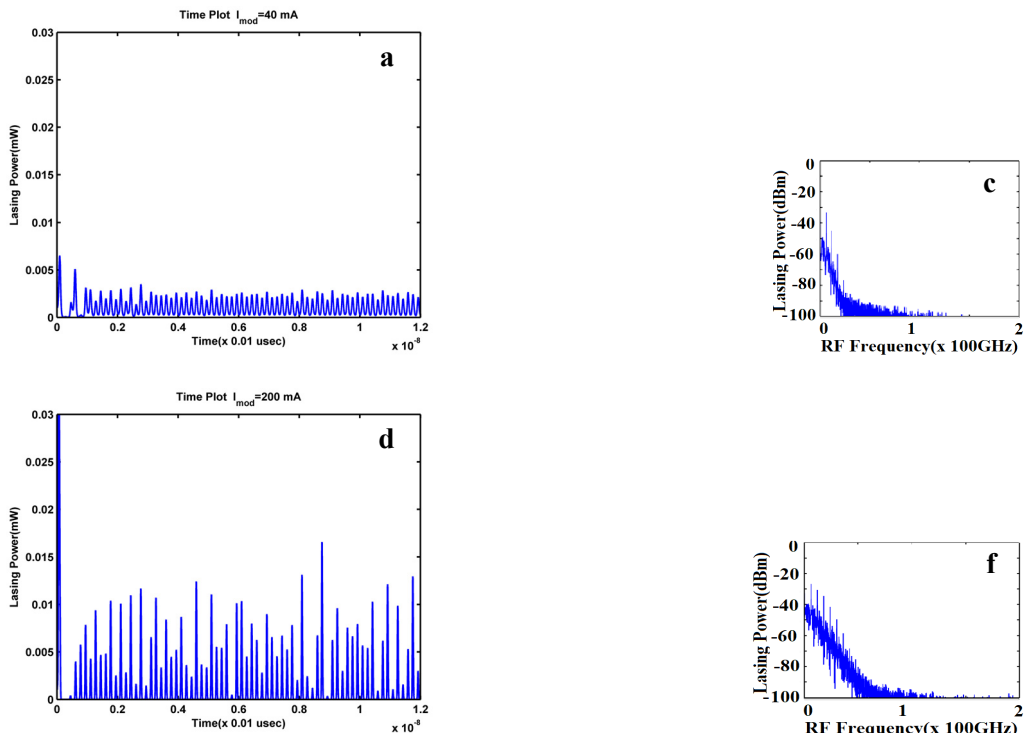


Fig. 2. Modulation current variation time, optical spectrum and RF spectrum. (a)–(c) 40 mA, (d)–(f) 200 mA, and (g)–(i) 400 mA

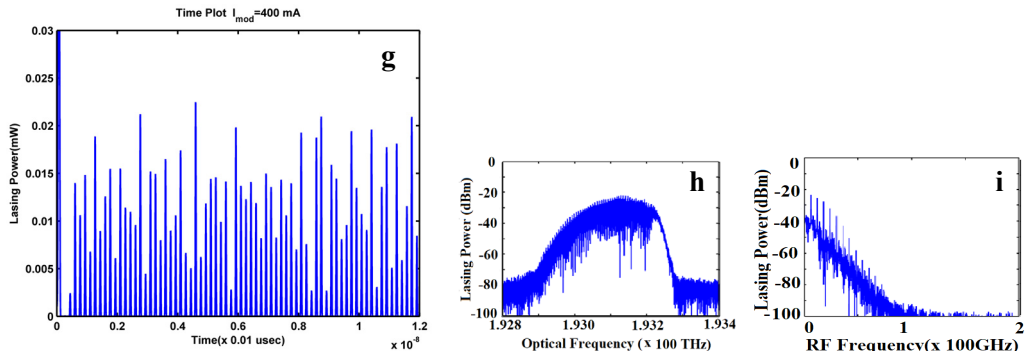


Fig. 2. Continued.

The mean, standard deviation and bandwidth results extracted out of 100 simulations for modulation current linearly increased from 40 to 400 mA are shown in Fig. 1. The bifurcation plot shown in Fig. 1a displays each occurring chaotic pulse peaks as one dot on a vertical line on value of control parameter, *i.e.*,  $I_{\text{mod}}$  in this case. It can be seen that the mean and dynamic range of chaos is increasing as the modulation current increases. It also signifies that the energy is spread all across in different amplitude. The mean value of chaotic pulse peak amplitudes is shown in Fig. 1b and is almost linearly increasing with  $I_{\text{mod}}$ . Figure 1c and 2d show dynamic range and standard deviation of chaos peak amplitude and both are almost same in this case. Figure 1d shows optical bandwidth, and it is also increasing with modulation current. The last graph is the measure of optical spectral energy pulses beyond 1.5 sigma limit.

### 3.2. Bias current $I_{\text{bias}}$

As the bias current is increased from 40 to 120 mA as per Fig. 3, the dynamic range of chaos is decreased. On the other hand, the bandwidth of chaos first decreases with bias current up to 65 mA and then increases. The decrease in bandwidth is attributed to decrease in modulation depth. However, the increase in bandwidth beyond bias current of 65 mA is of less use as the dynamic range of chaos is continuously becoming smaller in this range.

Figure 4 shows same five features using one hundred simulations for bias current linearly increased from 40 to 120 mA. Figure 4a shows increasing mean and decreasing dynamic range of chaos visible in bifurcation plot. Figure 4b shows the increasing mean of chaotic pulse peak amplitudes. Figure 4c and 4d show that dynamic range and standard deviation are first increasing and then decreasing, and both are almost same. Figure 4d shows optical bandwidth which reduces to minimum at  $I_{\text{bias}} = 65 \text{ mA}$ . The last graph is the measure of optical spectral energy pulses beyond 1.5 sigma limit. It reduces to 45% at 45 mA. The best chaos from application point of view is a particular application dependent because it depends on what weightage we give to dynamic range and energy outside the sigma limits.

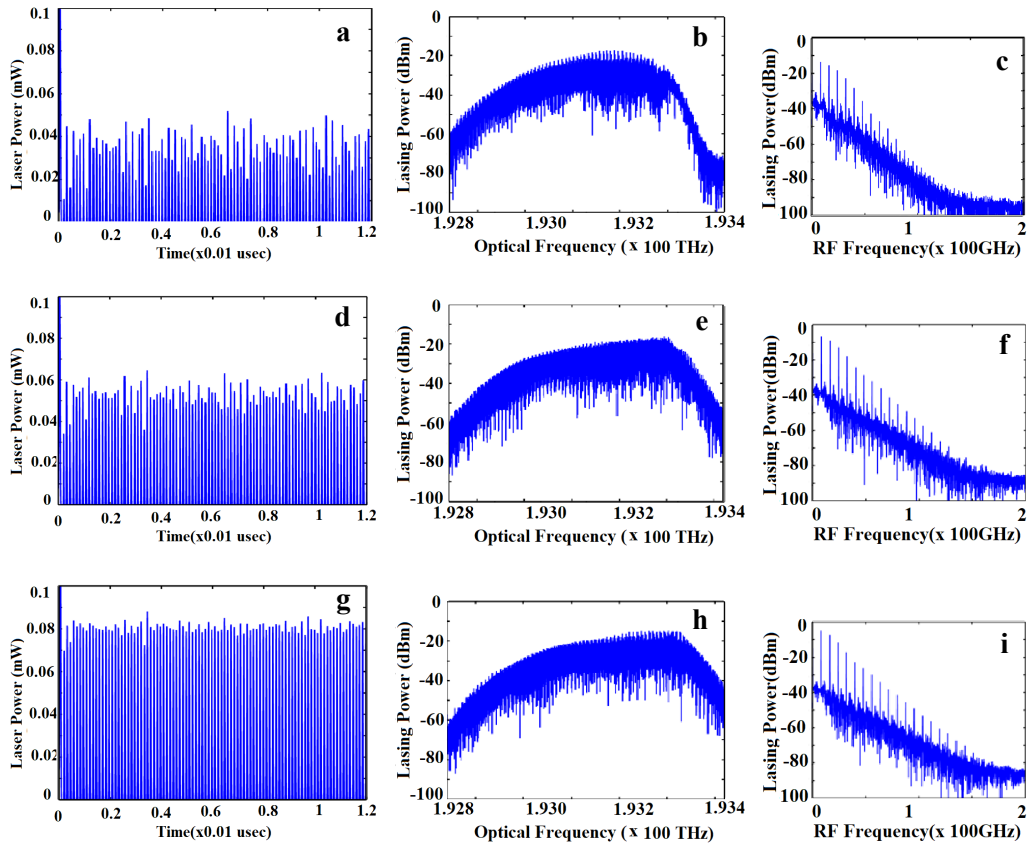


Fig. 3. Bias current variation time plots, optical spectrum and RF spectrum. (a)–(c) 60 mA, (d)–(f) 100 mA, and (g)–(i) 120 mA.

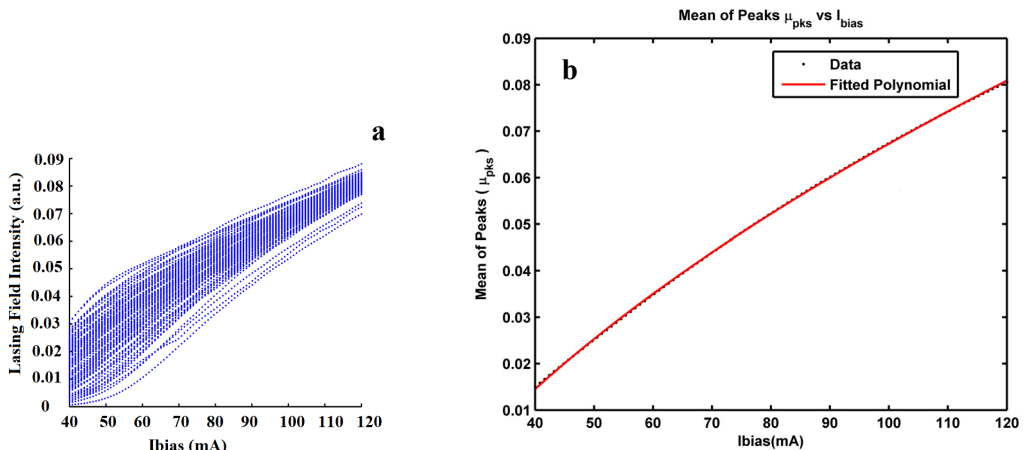


Fig. 4. Chaotic peaks variation with  $I_{\text{bias}}$ . (a) Bifurcation plot, (b) mean power, (c) standard deviation, (d) optical 10 dB bandwidth.

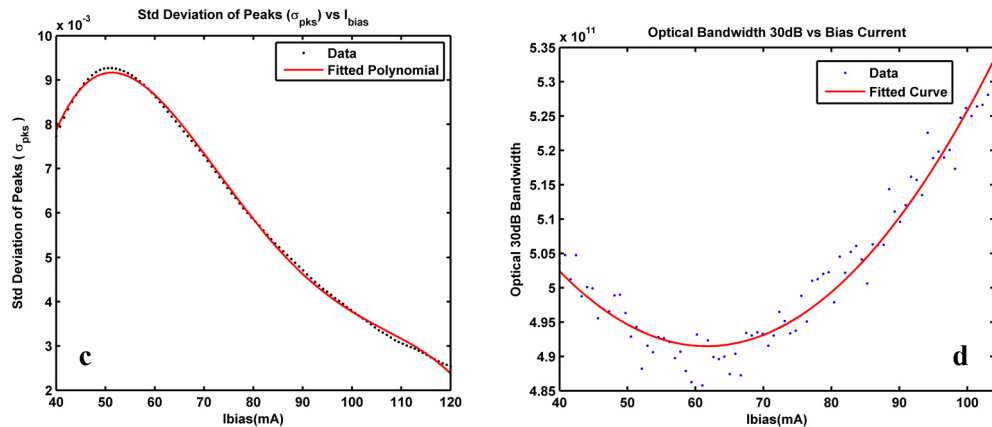


Fig. 4. Continued.

### 3.3. Modulation frequency $\omega_a$

The modulation frequency is increased from 4 to 15 GHz keeping rest of parameters as in the Table. The resulting time, optical and RF spectral plots are shown in Fig. 5.

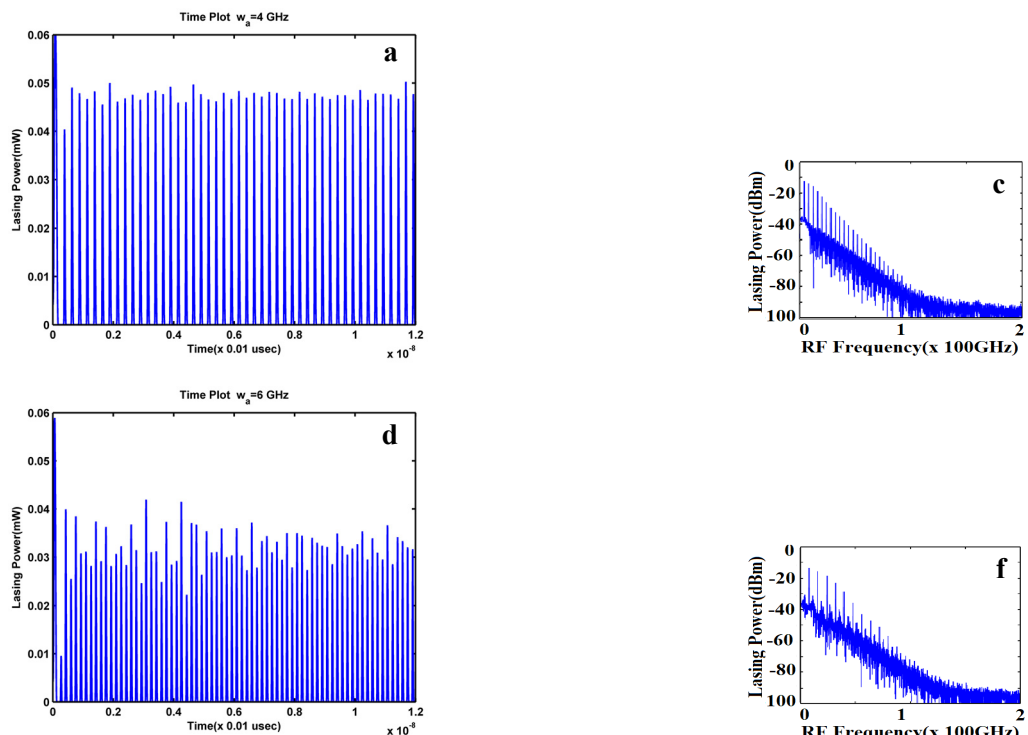


Fig. 5. Modulation frequency variation time, optical spectrum and RF spectrum. (a)–(c) 4 GHz, (d)–(f) 6 GHz, (g)–(i) 9 GHz.

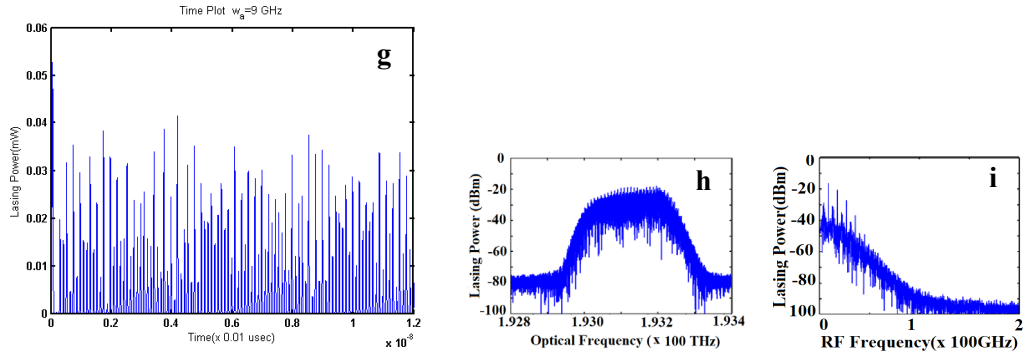


Fig. 5. Continued.

Initially the dynamic range and hence bandwidth of chaos are less at 4 GHz. The maximum pulse amplitude dynamic range and bandwidth are achieved at 9 GHz. Beyond 9 GHz which is the optimal or maxima point of bandwidth, the dynamic range and bandwidth start decreasing. The reasoning for the decrease in dynamic range and bandwidth with the increase in modulation frequency is that faster chaos generation dynamics demands a higher bias and modulation currents. So, for every set of bias and modulation current there will be one modulation frequency for maximum chaos bandwidth generation.

Figure 6 shows same five features utilizing one hundred simulations for modulation frequency linearly increased from 4 to 15 GHz. Figure 6a shows a decreasing mean and first increasing and then decreasing dynamic range of chaos visible in bifurcation plot. Figure 6b shows clearly the exponentially decreasing mean of chaotic pulse peak amplitudes with increasing modulation frequency because the laser cavity cannot support high amplitude pulses for same pump power as we try to create higher

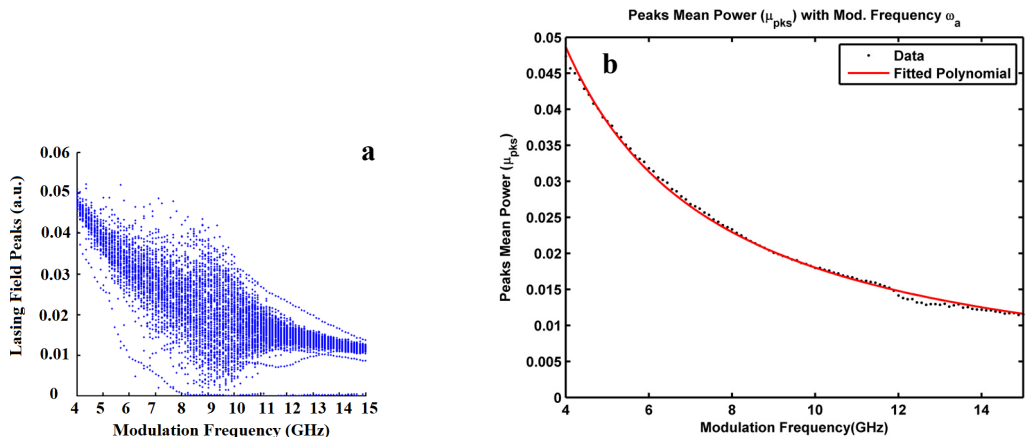


Fig. 6. Chaotic peaks variation with  $\omega_a$ . (a) Bifurcation plot, (b) mean power, (c) standard deviation, (d) optical 10 dB bandwidth.

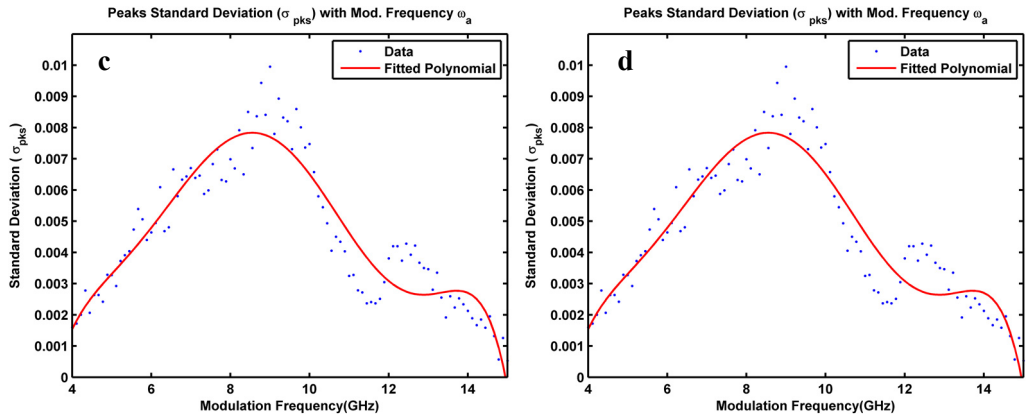


Fig. 6. Continued.

pulse repetition rates. Figures 6c and 6d show that dynamic range and standard deviation are increasing and then decreasing in similar fashion. Figure 6d shows optical bandwidth which rises to maximum at 7.5 GHz. Figure 6d is the measure of optical spectral energy pulses beyond 1.5 sigma limit and a threshold can be decided as per application requirement. The graph is first decreasing to reach a minima and then increasing.

#### 4. Discussion

A nonlinear system, like the directly modulated SL studied here, can move between stable, n-T pulsed periodic, quasi-periodic or chaos as per its bifurcation behavior by varying the control parameters. However, it may be noted that in all above simulations, the operating point of laser diode has been established in a region such that the laser does not move out of chaotic mode of operation once the parameter of interest is varied intentionally in a limited range. This way we can focus on temporal and spectral trend analysis with parameters being varied on a narrow range of interest. Also, the parameters are varied both one at a time to establish the trends. This condition was ensured in the beginning of this paper by showing the limited range bifurcation plots for three parameters with continuous retention of chaotic region.

It can be seen in general that the modulating frequency determines the maximum pulse repetition frequency and hence maximum optical and RF bandwidths of chaos. However, at higher modulation frequency, a higher bias current and higher modulation current are required and therefore there is always a maxima at which maximum bandwidth is attained. The modulation current measures the dynamic range of chaotic peaks. The bandwidth is found always increasing with modulation depth and modulation current. The bias current determines the peak and average power of chaotic pulses; however, increasing the bias current alone will reduce the modulation depth and decrease the bandwidth.

## 5. Conclusion

Establishing well-defined causal relation between chaos bandwidth and three control parameters using extensive simulations results is successfully achieved in this work. Optical chaos pulses peak and average pulse power, bandwidth, center frequency and overall spectral profile in a directly modulated semiconductor laser are varied w.r.t. bias current, modulation current and modulation frequency. Time domain, optical spectrum and RF spectrum plots are first discussed, and a qualitative visual analysis is done in simulations. Later statistical features are extracted and plotted for each parameter variation at 100 points. Regressed graphs are formed and plotted along with the data points. Our next logical future work is using optimization tools to select laser parameters for given RoF signal to design secure communication system for given link budget.

## References

- [1] MAZHAR D.A., SHAH S.Z.A., ISLAM M.K., QAMAR F., *Design issues of digital and analog chaotic RoF link using chaos message masking*, IEEE Access **7**, 2019, pp. 174042–174050, DOI: [10.1109/ACCESS.2019.2957255](https://doi.org/10.1109/ACCESS.2019.2957255).
- [2] SCIAMANNA M., SHORE K.A., *Physics and applications of laser diode chaos*, Nature Photonics **9**(3), 2015, pp. 151–162, DOI: [10.1038/nphoton.2014.326](https://doi.org/10.1038/nphoton.2014.326).
- [3] ARGYRIS A., SYVRIDIS D., LARGER L., ANNOVAZZI-LODI V., COLET P., FISCHER I., GARCÍA-OJALVO J., MIRASSO C.R., PESQUERA L., SHORE K.A., *Chaos-based communications at high bit rates using commercial fiber optic links*, Nature **438**(7066), 2005, pp. 343–346, DOI: [10.1038/nature04275](https://doi.org/10.1038/nature04275).
- [4] LIU H.-F., NGAI W.F., *Nonlinear dynamics of a directly modulated 1.55  $\mu$ m InGaAsP distributed feedback semiconductor laser*, IEEE Journal of Quantum Electronics **29**(6), 1993, pp. 1668–1675, DOI: [10.1109/3.234419](https://doi.org/10.1109/3.234419).
- [5] ILLING L., KENNEL M.B., *Shaping current waveforms for direct modulation of semiconductor lasers*, IEEE Journal of Quantum Electronics **40**(5), 2004, pp. 445–452, DOI: [10.1109/JQE.2004.826446](https://doi.org/10.1109/JQE.2004.826446).
- [6] ALI S.Z., ISLAM M.K., ZAFRULLAH M., *Effect of parametric variation on generation and enhancement of chaos in erbium-doped fiber-ring lasers*, Optical Engineering **49**(10), 2010, 105002, DOI: [10.1117/1.3491202](https://doi.org/10.1117/1.3491202).
- [7] ALI S.Z., ISLAM M.K., ZAFRULLAH M., *Generation of higher degree chaos by controlling harmonics of the modulating signal in EDFRL*, Optik **122**(21), 2011, pp. 1903–1909, DOI: [10.1016/j.ijleo.2010.11.022](https://doi.org/10.1016/j.ijleo.2010.11.022).
- [8] ALI S.Z., ISLAM M.K., ZAFRULLAH M., *Comparative analysis of chaotic properties of optical chaos generators*, Optik **123**(11), 2012, pp. 950–955, DOI: [10.1016/j.ijleo.2011.07.010](https://doi.org/10.1016/j.ijleo.2011.07.010).
- [9] ALI S.Z., ISLAM M.K., ZAFRULLAH M., *Effect of message parameters in additive chaos modulation in erbium doped fiber ring laser (EDFRL)*, Optik **124**(18), 2013, pp. 3746–3750, DOI: [10.1016/j.ijleo.2012.11.027](https://doi.org/10.1016/j.ijleo.2012.11.027).
- [10] ALI S.Z., ISLAM M.K., *Erbium-doped fiber ring laser dynamical analysis for chaos message masking scheme*, Optica Applicata **47**(3), 2017, pp. 395–410, DOI: [10.5277/oa170306](https://doi.org/10.5277/oa170306).
- [11] GOMES N.J., MONTEIRO P.P., GAMEIRO A., *Next Generation Wireless Communications Using Radio Over Fiber*, Wiley, 2012.
- [12] JUANG C., HWANG T.M., JUANG J., LIN W.W., *Optical chaotic AM demodulation by asymptotic synchronization*, IEEE Photonics Technology Letters **12**(2), 2000, pp. 179–181, DOI: [10.1109/68.823509](https://doi.org/10.1109/68.823509).

- [13] CHONGFU ZHANG, QIAOYANZHANG, YINGWANG, KUNQIU, BAOJIANWU, CHANGCHUNLI, *Proposal for 60 GHz wireless transceiver for the radio over fiber system*, Optics & Laser Technology **56**, 2014, pp. 146–150, DOI: [10.1016/j.optlastec.2013.07.026](https://doi.org/10.1016/j.optlastec.2013.07.026).
- [14] XIUPUZHANG, TAIJUN LIU, DONGYA SHEN, *Investigation of broadband digital predistortion for broadband radio over fiber transmission systems*, Optics Communications **381**, 2016, pp. 346–351, DOI: [10.1016/j.optcom.2016.07.025](https://doi.org/10.1016/j.optcom.2016.07.025).
- [15] BOUCHEZ G., MALICA T., WOLFERSBERGER D., SCIAMANNA M., *Manipulating the chaos bandwidth of a semiconductor laser subjected to phase-conjugate feedback*, Proc. SPIE 11356, Semiconductor Lasers and Laser Dynamics IX, 2020, 113560Y, DOI: [10.1117/12.2559627](https://doi.org/10.1117/12.2559627).
- [16] SCHIRES K., GOMEZ S., GALLET A., DUAN G.H., GRILLOT F., *Passive chaos bandwidth enhancement under dual-optical feedback with hybrid III-V/Si DFB laser*, IEEE Journal of Selected Topics in Quantum Electronics **23**(6), 2017, 1801309, DOI: [10.1109/JSTQE.2017.2732830](https://doi.org/10.1109/JSTQE.2017.2732830).
- [17] QUIRCE A., VALLE Á., THIENPONT H., PANAJOTOV K., *Enhancement of chaos bandwidth in VCSELs induced by simultaneous orthogonal optical injection and optical feedback*, IEEE Journal of Quantum Electronics **52**(10), 2016, 2400609, DOI: [10.1109/JQE.2016.2605400](https://doi.org/10.1109/JQE.2016.2605400).
- [18] NIANQIANG LI, WEI PAN, SHUIYING XIANG, LIANSHAN YAN, BIN LUO, XIHUA ZOU, LIYUE ZHANG, *Bandwidth and unpredictability properties of semiconductor ring lasers with chaotic optical injection*, Optics & Laser Technology **53**, 2013, pp. 45–50, DOI: [10.1016/j.optlastec.2013.04.026](https://doi.org/10.1016/j.optlastec.2013.04.026).

Received April 22, 2021